Materials Letters 150 (2015) 114–117

Contents lists available at ScienceDirect

Materials Letters

journal homepage: www.elsevier.com/locate/matlet

Preparation and characterization of chitosan hollow nanospheres for anticancer drug curcumin delivery

Mingxian Liu*, Jing Yang, Peng Ao, Changren Zhou

Department of Materials Science and Engineering, Jinan University, Guangzhou 510632, China

ARTICLE INFO

Article history:
Received 1 February 2015
Accepted 5 March 2015
Available online 11 March 2015

Keywords:
Nanoparticles
Polymers
Microstructure

ABSTRACT

Chitosan hollow nanospheres (CHNs) with diameter of 500–1000 nm and opening of 300–500 nm are synthesized via solid–liquid phase separation. The chemical composition, crystal structure, morphology, size and pore property, and the formation condition of the nanospheres have been examined. The CHNs have a specific surface area of 101.91 m^2/g and show mesopores and macropores on their interior and outer surfaces. The methyl-thiotetrazole assay proves the low cytotoxicity of the CHNs. The CHNs show the maximum 63.9 wt% of the anticancer curcumin drug loading capacity. 87% of the loaded curcumin is released from the nanospheres over 50 h. The CHNs show potential applications in drug/gene delivery for cancer therapy.

1. Introduction

Hollow nanospheres or nanocapsules are an important branch of nanostructure materials. Due to their unique physical and chemical properties, such as low density, high specific surface area, better permeability, and encapsulation of guest molecules, hollow nanospheres show potential applications in targeted drug delivery and advanced functional materials [1,2]. Among them, the hollow polymeric nanospheres can encapsulate large quantities of therapeutic and diagnostic agents in their hollow inner cavities and release them at later stage [3,4]. Such encapsulation can greatly increase drug bioavailability, protect against degradation factors like pH and light, and modify their pharmacokinetics and biodistribution in body [5]. Numerous methods, such as deposition on templates, self-assembly, microemulsion polymerization, and pH-induced micellization, have been employed to synthesize hollow polymeric nanospheres [6–8]. However, the removing the templates to create hollow interior is complicated and energy consuming. Usage of large amount surfactants also induces the potential toxicity for cells and tissue. A simple and versatile method without using surfactants is therefore needed.

Among the polymers for preparation of nanospheres, chitosan (CS) is a good candidate because of its many potential applications in biomedical areas such as the drug delivery carriers [9–11]. The chitosan hollow nanospheres (CHNs) can be fabricated by employing poly-D,L-lactide–poly(ethylene glycol) nanoparticles as templates [12]. Hollow CS–poly(acrylic acid) (CS–PAA) nanospheres with an outer shell of positively charged CS chains and an inner shell of CS–PAA polyelectrolyte complexes can also be prepared by polymerization of acrylic acid upon addition of initiator to an aqueous solution of chitosan–acrylic acid solution [13]. The CS–PAA nanospheres had a continuous release of the entrapped DOX up to 10 days *in vitro* [14].

To the best of our knowledge, no study has been reported on the preparation of hollow nanosphere of pure chitosan. Here, we present a simple solid–liquid phase separation method for fabricating CHNs with controlled size and featured drug delivery property. The chemical composition, crystal structures, morphologies, sizes, pore properties, the formation conditions, and drug loading ability of the nanospheres were studied. The prepared CHNs show potential of applications for drug/gene delivery for cancer therapy.

2. Materials and methods

Materials: Chitosan was supplied by Jinan Haidebei Marine Bioengineering Co., Ltd (China). Its deacetylation and viscosity–average molecular weight were 95% and 600,000 g/mol, respectively. Acetic acid and other chemicals used in this paper were analytical grade. Ultrapure water from Arium 611 Ultrapure Water Systems (Sartorius, Germany) was used to prepare the aqueous solutions.

Solid–liquid phase separation method for preparation of CHNs: 0.05% (w/v) CS solution was prepared by dissolving 5.0 mg chitosan in 10 mL 0.025% (v/v) acetic acid aqueous solution at room temperature. Then, the solution (1.5 mL) placed in a plastic

* Corresponding author.
E-mail address: liumx@jnu.edu.cn (M. Liu).

http://dx.doi.org/10.1016/j.matlet.2015.03.013
0167-577X/

tube (12 mm diameter × 50 mm height) was quickly immersed into liquid nitrogen for 2–24 h. The frozen samples were then freeze-dried under −80 °C using Christ freeze dryer ALPHA 1-2/LD plus. This process allowed the preparation of CS samples with geometries of hollow nanospheres or micro(nano)-fibers.

Characterization: The samples were dried thoroughly and kept in desiccators before analysis. FTIR spectra were measured between 400 and 4000 cm^{-1} on a MAGNA-IR760 (Nicolet Co., USA) infrared spectrometer. X-ray powder diffraction (XRD) experiment was conducted using X-ray diffractometer (D8, Bruker Corporation) equipped with Cu-κα radiation. The morphology of the nanospheres was observed with a Zeiss Ultra 55 scanning electron microscopy and Philips TECNAI 10 transmission electron microscopy. The Brunauer–Emmett–Teller (BET) surface area and pore structure of the nanospheres were investigated using the nitrogen adsorption method with Quantachrome ASIQACIV200-2.

Cytotoxicity by MTT assay: MC-3T3 cells were grown in RPMI medium 1640 with 10% FBS. The cells were seeded at a density of 1×10^4 cells per well in 1.5 mL of medium in 24-well plates and grown for 12 h. The cells were then exposed to the CHNs at different concentrations. Cell viability was measured using the 3-(4,5-dimethylthiazol-2-yl)-2,5-diphenyltetrazolium bromide (MTT) method. The polystyrene plates were used as control. The data were estimated from three individual experiments, and the standard deviation was calculated.

Curcumin loading and release studies: A certain amount of CHNs were added into the curcumin ethanol solution. The solution was stirred for 1 h followed by centrifugation (3489*g*, 5 min) and freeze-dried. The supernatant was decanted by the microplate reader at the absorbance of 405 nm. Curcumin encapsulated CHNs were placed in PBS buffer (pH 7.4) at 37 °C. Curcumin released from the nanospheres was evaluated by partitioning a small aliquot of the release mixture at various time points.

3. Results and discussions

The solid–liquid phase separation occurred during the freezing process is a generic method for preparation of nanostructure [2,15]. Freezing the chitosan solution causes constitutional supercoiling at CS molecular chains and the water interface, leading to Mullins–Sekerka instability and ice cell growth into a well-defined structure. The chemical composition of the prepared CHNs was firstly investigated by the FTIR technique (Fig. 1(A)). It can be seen that the CHNs show typical absorbance peaks of chitosan in the region of 3010–3650 cm^{-1} (N–H and O–H), 2970–2840 cm^{-1} (C–H), 1640 cm^{-1} (amide I vibration band, C–O stretch of acetyl group) and 1555 cm^{-1} (amide II band, N–H stretch) [16]. The shape and location of the peaks for the raw CS and CHNs are same, indicating the absence of chemical reactions during solid–liquid phase separation. The X-ray diffraction of the raw CS shows two characteristic peaks at around $2\theta = 11.28°$ and at $2\theta = 21.18°$ (Fig. 1(B)). After being prepared into nanospheres, the CS shows two similar diffraction peaks but with decreased intensity. This is due to that part of the crystallized CS may transfer into amorphous state during the phase separation process. Fig. 1(C) is a typical SEM image of the CHNs. It clearly shows the prepared CHNs have diameters of 500–1000 nm. The CHNs have hollow interior as revealed by high-magnification SEM images in Fig. 1(D). The CHNs have bowl shape morphology with an opening of 300–500 nm in diameter on their surface. However, some relatively small spheres can also be seen in the samples; these can be attributed to the polydispersity of the molecular weight of CS. Part of the shells of the nanospheres shrink into imperfect spherical shape. Nevertheless, the solid–liquid phase separation is a good method for preparation of CHNs, since it is a template-free and surfactants-free process.

The experiment parameters to influence the formation of the CHNs, such as the concentration of the CS solution and the freezing time of the solution, were investigated. The morphology of the freeze-dried product changes from the fiber-like structures to hollow nanospheres with the increase in the CS concentration up to 0.05% (Fig. 2(A)–(D)). The 0.05 (w/v) CS and 0.025% (v/v) acetic acid are the optimal ratios for obtaining the best hollow nanospheres morphology. Beyond the 0.05% CS concentration, the lyophilized product further becomes disordered micro (nano)-fibers, which has also been reported by Zhao et al. [17]. The freezing time also affects the morphology of the nanospheres (Fig. 2(E)–(H)). Freezing of the solution with 13 h leads to the hollow nanosphere with the uniform morphology for the 0.05% CS concentration. Too short or too long freezing leads to nano-/micro-fibrous structure. The CHNs may have high drug loading ability and subsequently sustained drug delivery property compared with the CS nanofibres due to their large interior empty structures. The shells can restrict the encapsulated drug molecules going out of the nanospheres freely.

TEM images also reveal the hollow interior of the CHNs. The TEM examinations (Fig. 3 inset) present the same size range as the results of SEM observation. Thus, it seems safe to conclude that the prepared CHNs with diameter of 500–1000 nm have hollow interior with opening of 300–500 nm. The surface area analysis was carried out on the CHNs by the BET method. The specific surface area is determined as 101.91 m^2/g. The nitrogen sorption isotherms of the CHNs are depicted in Fig. 3(A), showing Type IV adsorption with a Type H3 hysteresis loop. The Type H3 loop is usually observed with aggregates of plate-like particles giving rise to slit-shaped pores. There are slit-shape pores on the surfaces of the prepared CHNs as shown from the high-magnification SEM images. The BJH pore size distribution curve of the CHNs is shown in Fig. 3(B). The pore size ranges from 3 to 120 nm, which indicates there are mesopores and macropores. The CHNs show peaks at 4–10 nm, and a high peak around 100 nm which is attributed to the surface defects and the open pores of the CHNs, respectively. The presence of pores on the surfaces of the hollow spheres is useful for the adsorption of drugs.

Cytotoxicities of the CHNs were evaluated using MTT assay with cultured osteoblast-like cells (MCT-3T3-E1). Fig. 3(C) reveals the cytotoxicity of the CHNs after 4 h culture. It can be seen that the nanospheres nearly do not show the cytotoxicity with low concentration (2 mg/mL). With the increase of the nanospheres concentration, decreased cell viability is found. However, the cell viability is still higher than 50% even at the highest nanosphere concentration (16 mg/mL). To investigate the drug-loading capacity and drug-release behavior of the CHNs, the curcumin was loaded into the nanospheres and released in PBS buffer. The effect of weight ratio of CS and curcumin on entrapment efficiency and loading capacity is shown in Table 1. It can be seen that the entrapment efficiency and loading capacity of the drug increase with the increase of the ratio of CS and curcumin. The optimal recipe of the CS and curcumin is 1:1 at which the entrapment efficiency and the loading capacity are 63.93% and 52.33%, respectively. Fig. 3(D) shows the curcumin release profiles of the CHNs. In the first 12 h, the release is burst and 48.67% of the drug is released from the nanospheres. This stage can be attributed to the release of curcumin absorbed on the outer surface of the nanospheres. In the period of 12–48 h, the release rate decreases. This can be attributed to the releasing of the curcumin wrapped in the interior of the nanospheres. With further prolonging of releasing time, the release rate becomes lower. At 120 h, the releasing ratio reaches 94%. The sustained release of the curcumin is obviously better that that in the CS solid nanoparticles in which the release of the curcumin was complete within 2 h [18]. Therefore, the prepared CHNs have a good entrapping ability and controlled releasing behavior of the curcumin.

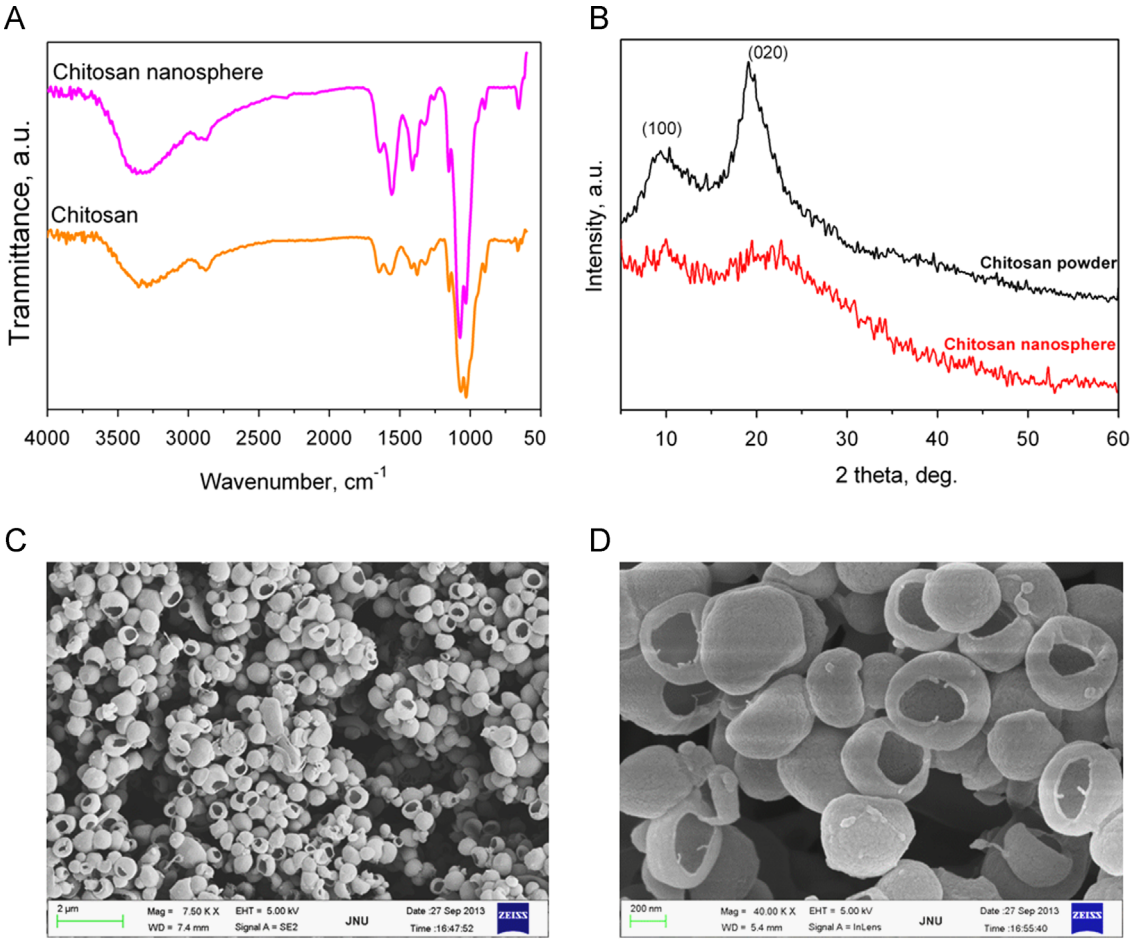

Fig. 1. FTIR spectra (a), XRD pattern (b), SEM photos ((c) and (d)) of CHNs.

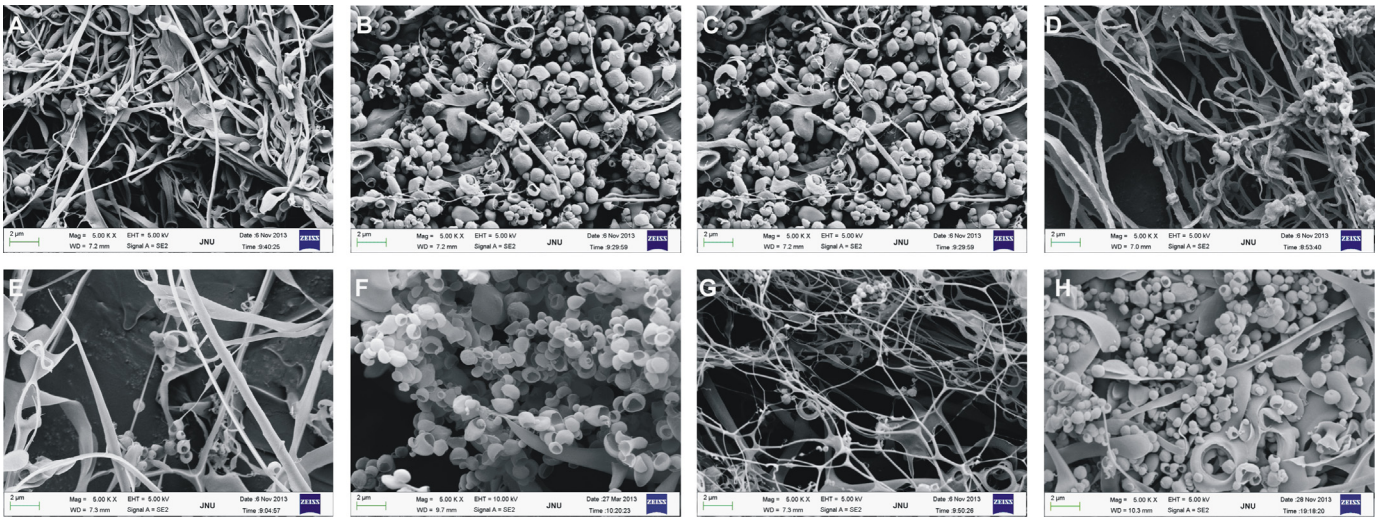

Fig. 2. Influence of CS solution concentration and freezing time on the morphology of the nanospheres. The CS concentration of (A)–(D) was 0.0125, 0.025, 0.05, 0.1 g in 25 μL acetic acid/100 mL water with 24 h freezing. The CS concentration of (E)–(H) was 0.05 g chitosan in 25 μL acetic acid/100 mL water with 1, 13, 24, 48 h freezing.

4. Conclusions

The CHNs with diameter of 500–1000 nm can be prepared via solid–liquid phase separation method. FTIR and XRD results confirm the chemical composition and crystal structure of the CHNs. The CS solution concentration and the freezing time have significant effects on the morphology of the nanospheres. The CHNs have a specific surface area of 101.91 m^2/g and show mesopores and macropores on their interior and outer surfaces. The CHNs have low cytotoxicity as determined by culturing of osteoblast cells. CHNs have a good entrapping ability and controlled releasing behavior of the curcumin drug. Although the size

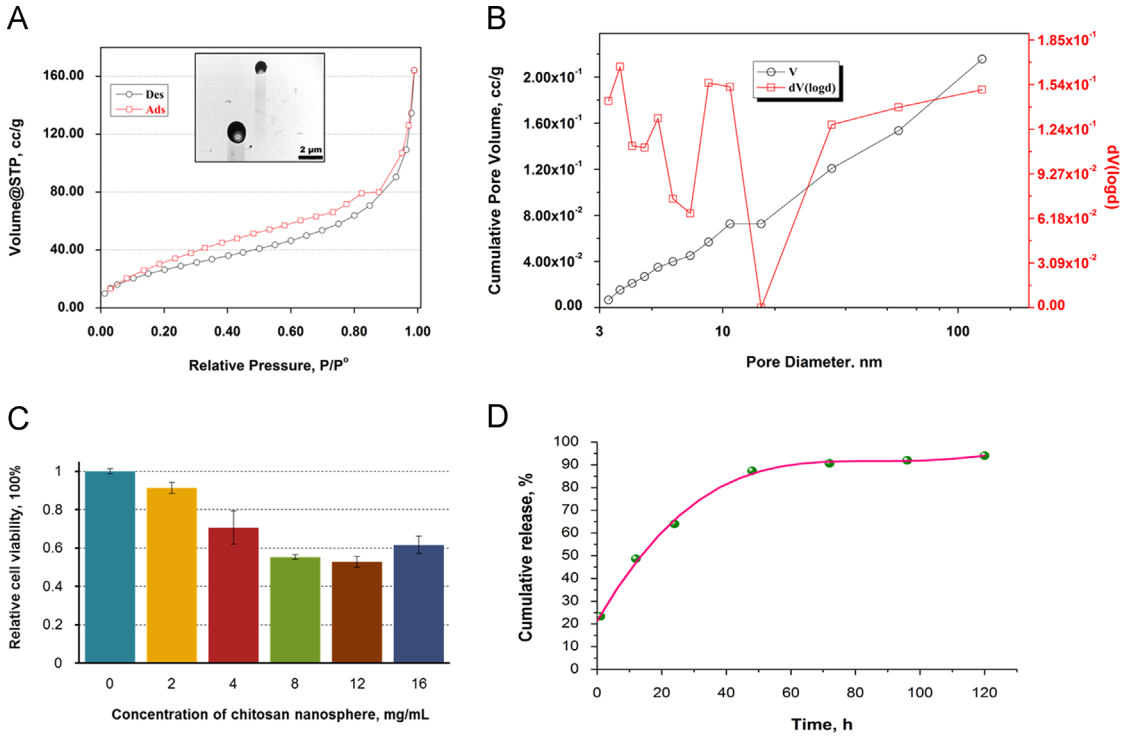

Fig. 3. Nitrogen adsorption–adsorption isotherms (A) and BJH pore size distribution (B) curves of the CHNs. The inset in (A) is the TEM photos of the CHNs; MC-3T3 cell viability of CHNs (C) and the typical *in vitro* release profile of curcumin loaded CHNs at 37 °C (D).

Table 1
Effects of weight ratio of CS and curcumin on entrapment efficiency and loading capacity of CHNs.

Weight ratio of CS and curcumin	Entrapment efficiency (%)	Loading capacity (%)
1:0.2	0.38	0.06
1:0.5	57.13	19.04
1:1	63.90	63.93
1:2	70.65	47.10
1:4	75.60	58.08

uniformity needs to be improved in the future work, this new type of CHNs will attract a range of interesting studies related to drug encapsulation and delivery for cancer therapy.

Acknowledgment

This work was financially supported by the National Natural Science Foundation of China (Grant no. 51473069), the Guangdong Natural Science Funds for Distinguished Young Scholar (Grant no. S2013050014606), and the Special Fund for Ocean-Scientific Research in the Public Interest (201405105).

References

[1] Hu Y, Jiang X, Ding Y, Chen Q, Yang CZ. Adv. Mater. 2004;16(11):933.
[2] Im SH, Jeong UY, Xia YN. Nat Mater 2005;4(9):671.
[3] Hu Y, Chen Y, Chen Q, Zhang L, Jiang X, Yang C. Polymer 2005;46(26):12703.
[4] Yuan X, Zhu B, Ma X, Tong G, Su Y, Zhu X. Langmuir 2013;29(39):12275.
[5] Mora-Huertas CE, Fessi H, Elaissari A. Int J Pharm 2010;385(1–2):113.
[6] Huang H, Remsen EE, Kowalewski T, Wooley KL. J Am Chem Soc 1999;121(15):3805.
[7] Wong MS, Cha JN, Choi K-S, Deming TJ, Stucky GD. Nano Lett 2002;2(6):583.
[8] Fleming MS, Mandal TK, Walt DR. Chem Mater 2001;13(6):2210.
[9] Liu M, Shen Y, Ao P, Dai L, Liu Z, Zhou C. RSC Adv 2014;4(45):23540.
[10] Liu M, Wu C, Jiao Y, Xiong S, Zhou C. J Mater Chem B 2013;1(15):2078.
[11] Liu M, Zhang Y, Wu C, Xiong S, Zhou C. Int J Biol Macromol 2012;51(4):566.
[12] Wang W, Luo C, Shao S, Zhou S. Eur J Pharm Biopharm 2010;76(3):376.
[13] Hu Y, Chen Q, Ding Y, Li RT, Jiang XQ, Liu BR. Adv Mater 2009;21(36):3639.
[14] Hu Y, Ding Y, Ding D, Sun M, Zhang L, Jiang X, Yang C. Biomacromolecules 2007;8(4):1069.
[15] Zhang H, Hussain I, Brust M, Butler MF, Rannard SP, Cooper AI. Nat Mater 2005;4(10):787.
[16] Schiffman JD, Schauer CL. Biomacromolecules 2006;8(2):594.
[17] Zhao J, Han W, Chen H, Tu M, Zeng R, Shi Y, Cha Z, Zhou C. Carbohydr Polym 2011;83(4):1541.
[18] OToole MG, Henderson RM, Soucy PA, Fasciotto BH, Hoblitzell PJ, Keynton RS, Ehringer WD, Gobin AS. Biomacromolecules 2012;13(8):2309.